Available online at www.sciencedirect.com
ScienceDirect
Quaternary Research 69 (2008) 276–291
QUATERNARY RESEARCH
www.elsevier.com/locate/yqres

Evidence for multiple, episodic, mid-Holocene Hypsithermal recorded in two soil profiles along an alluvial floodplain catena, southeastern Tennessee, USA

Steven G. Driese [a,*], Zheng-Hua Li [b], Larry D. McKay [b]

[a] Department of Geology, One Bear Place #97354, Baylor University, Waco, TX 76798-7354, USA
[b] Department of Earth and Planetary Sciences, University of Tennessee, Knoxville, TN 37996-1410, USA

Received 15 August 2007
Available online 7 February 2008

Abstract

Floodplain soil–paleosol successions are valuable archives for reconstructing Pleistocene–Holocene climate changes but have been relatively unstudied in the southern Appalachian region. Two soil profiles on a small floodplain in southeastern Tennessee, USA were described and sampled in detail using both pedological and geological approaches, including stable carbon isotope analysis of soil organic matter (SOM). Correlation between the 2 profiles was constrained by uncalibrated AMS ^{14}C ages of bulk humates, and using SOM $\delta^{13}C$ values, both mobile and immobile elements. Four distinct 2.5–4‰ shifts towards less negative $\delta^{13}C$ values for SOM suggest ~300-yr cyclicity and transient warmer and drier climate events, with either water-stressed C_3 vegetation or as much as 35% C_4 plants present during the mid-Holocene. These postulated multi-episodic drier climate conditions have never before been documented in the southern Appalachian region and are tentatively correlated with mid-Holocene warming and drying in the eastern US, the nearly time-equivalent mid-Holocene events documented in Texas, the US High Plains and in the Gulf of Mexico. High rates of floodplain sediment accumulation (0.5–3 mm/yr), high clay content and maintenance of poorly drained soil conditions favor preservation of high-resolution climate archives in floodplain deposits by inhibiting oxidation and translocation of organic C.

Keywords: Paleoclimate; Mid-Holocene soils; Stable carbon isotopes; Southeastern US; Floodplains

Introduction

The expression (i.e., onset, duration, frequency and intensity) of major Pleistocene to Holocene climate events, such as the Younger Dryas or the mid-Holocene Hypsithermal, is still poorly understood in the southeastern US, particularly for the inland southern Appalachian region. Lack of high-resolution paleoclimate proxy records for the southeastern US forces paleoclimate modelers to base their interpretations of paleoclimate in this region on better-understood regions of North America (e.g., northeastern and upper Midwestern US; Harrison et al., 2003) with considerable risk of misinterpreting climate in the Valley and Ridge province. The mid-Holocene warm period, or Hypsithermal, which shows variable structure in the continental US, is a significant case in point; evidence suggests that drought conditions prevailed in the southwestern and the mid-continent regions during the mid-Holocene "Altithermal" (Boutton et al., 1993; Nordt et al., 1994), whereas the US eastern seaboard may have had increased levels of precipitation (Webb et al., 1993; Leigh and Feeney, 1995; Dwyer et al., 1996; Goman and Leigh, 2004). Floodplain soils and sediments in the southern Appalachian region offer great potential for reconstructing Pleistocene–Holocene climate but have generally been underutilized (see summary in Driese et al., (2005)).

As a case study to test the utility of southern Appalachian floodplain soils as Holocene climate archives, we here characterize the close spatial variability of two mid-Holocene soils, both USDA Alfisols (aquic Hapludalfs to Epiaqualf or Endoaqualfs in USDA Soil Taxonomy) that experience seasonal saturation ("top–down" episaturation or "bottom–up" endosaturation, in an overall udic moisture regime and aquic conditions), using high-resolution sampling and integrated field, micromorphologic, and geochemical investigations. Soils developed 150 m apart on a small alluvial floodplain surface in which there is only 10-cm difference in elevation, and formed under the same climate and from the same parent material. In spite of apparent similarities in soil-forming factors, the two soils differ in their field morphology, micromorphology, and geochemistry due to differences in soil

* Corresponding author. Fax: +1 254 710 2673.
E-mail address: Steven_Driese@baylor.edu (S.G. Driese).

0033-5894/$ - see front matter © 2007 University of Washington. All rights reserved.
doi:10.1016/j.yqres.2007.12.003

drainage and depositional textures, subtle differences in topography (floodplain vs. channel), and major differences in hydrology (flood vs. slackwater). The primary objective of this study is to show that high-resolution stable isotope analysis of soil organic matter (SOM), combined with micromorphological evidence, can be useful for identifying transient high-frequency climate shifts related to warming and drying, and that floodplains with high sediment accumulation rates, high clay contents, and maintenance of organic C pools due to wetness are potentially valuable paleoclimate archives. We also postulate that other floodplains should be investigated in a similar manner to build a broader-scale and integrated record using our methodology in order to reconstruct Pleistocene–Holocene paleoclimates, especially in the southeastern US.

Location and setting

The study site is located on the floodplain of Savannah Creek, a tributary stream that flows southwestward into Chickamauga Lake (reservoir formed by impounded Tennessee River) in Hamilton County, southeastern Tennessee, US (Fig. 1). Floodplain sediments consist of a 3–3.5 m thick succession of alluvial deposits, deposited directly upon the Chickamauga Limestone (Middle Ordovician) and within 200–220 m elevation in a 2–3 km wide valley that strikes NE–SW (Luther, 1979). Broad, highly dissected ridges underlain by Knox Group (Cambro-Ordovician) cherty dolostones (elevation averages 250–300 m) dominate the drainage basin to the northwest of the study site, whereas Rockwood Formation (Lower Silurian) quartz-rich sandstones form a higher relief (average elevation 350–400 m) source region for alluvium to the southeast (Fig. 1). Soils have developed in the alluvial parent materials and evidence of pedogenic processes extends to depths of 130–170 cm.

The surface of the field area has a slope less than 1%, and elevation is estimated as ~210 m, based on the Snow Hill, TN 7.5′ USGS topographic map and hand-held GPS measurements. It is currently utilized for hay and pasture, and the vegetation consists of fescue, sedges, ironwood, chickweed, red clover, and white clover, although bottomland hardwoods probably dominated the vegetation prior to anthropogenic disturbance. Somewhat poorly drained to poorly drained conditions characterize the field area, which is intermittently flooded by Savannah Creek located 0.4 km to the east of the site.

Climate at the study site is temperate and humid, with hot summers and cool winters. Mean annual precipitation averages about 1330 mm, generally evenly distributed throughout the year; October is the driest month, whereas March is the wettest month (Jackson, 1982). For the period 1890–2003, monthly MAP demonstrates 5- to 7-yr cycles alternating between wet and dry periods (National Climatic Data Center, Asheville, NC: http://lwf.ncdc.noaa.gov/oa/ncdc.html). For the same period of record, mean annual temperature averages 15.3°C. Soils at the site are mapped as the Tupelo and Ketona series; type descriptions are accessible through the USDA Natural Resource Conservation Service, Soil Series Classification Data Access at: http://soils.usda.gov/technical/classification/scfile/index.html.

Soil parent material is fine-textured alluvium derived predominantly from limestone.

Methods

Two 2–2.5-m-deep by 3-m-long soil pits were excavated with a backhoe on a floodplain of Savannah Creek in Hamilton County, near Ooltewah, southeastern Tennessee (Fig. 1). At the time of excavation the floodplain was wet, with some pools of standing water and water flowing within a small drainage ditch transecting the floodplain; water began to infiltrate the Ketona soil pit immediately after excavation, derived from both surface ponding and seepage from depth, and a gasoline-powered pump was necessary to remove water during soil description and sampling. Soils were described and soil horizons defined using standard pedological techniques (Soil Survey Staff, 1998; Table 1). Bulk soil samples of about 200 g were collected at 10-cm intervals to the base of each pit. The Tupelo profile was sampled down to the contact with Middle Ordovician limestone bedrock (270 cm), whereas the Ketona profile was only sampled to 170 cm due to standing water, and buckets of deeper soil material were sampled to a bedrock

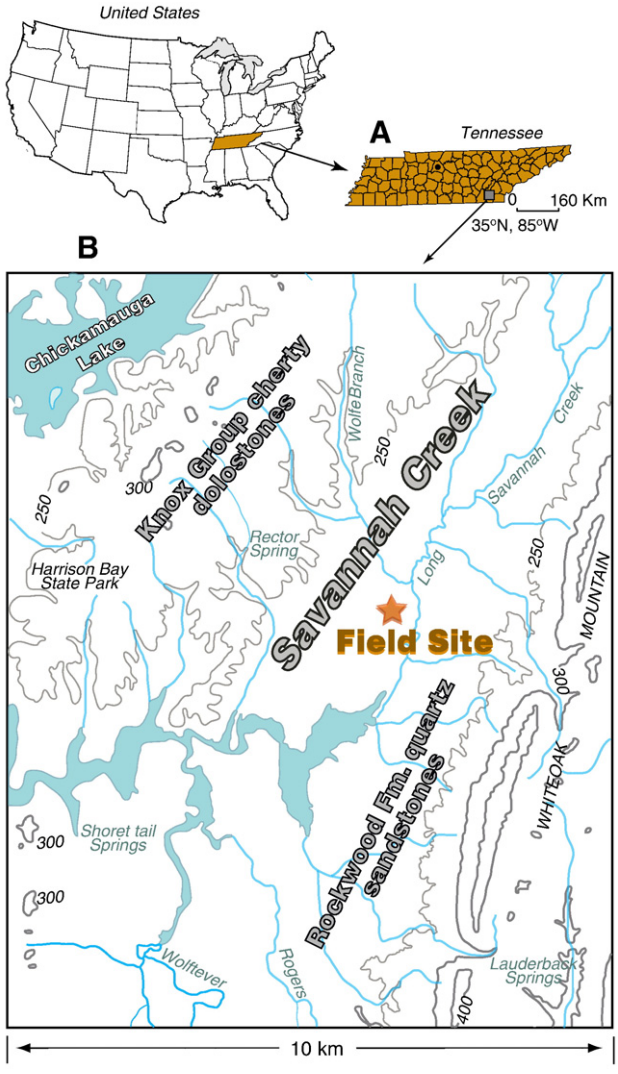

Figure 1. Location of soil sampling site on alluvial floodplain in Hamilton County in southeastern Tennessee, based on Chattanooga (1979) 1:100,000 metric map base, 50-m contour interval. Floodplain soils and sediments directly overlie Chickamauga Group (Middle Ordovician) limestone deposits.

https://doi.org/10.1016/j.yqres.2007.12.003 Published online by Cambridge University Press

Table 1
Soil descriptions (corrected to laboratory data)

Tupelo clay to silty clay loam (USDA-NRCS pedon code: S02-TN-065-1)

Ap—(0 to 20 cm); light olive brown (2.5Y 5/3) silty clay loam; moderate medium granular structure; very friable; many fine and medium roots; few fine prominent black (10YR 2/1) manganese concretions; 1 percent rounded gravel; moderately acid; gradual smooth boundary.

BE—(20 to 33 cm); dark yellowish brown (2.5Y 5/4) silty clay loam; moderate fine subangular blocky structure; friable; slightly sticky, slightly plastic; many very fine and fine, roots; common medium distinct grayish brown (2.5Y 5/2) iron depletions; common fine prominent yellowish brown (10YR 5/8) masses of iron accumulation; common fine prominent black (10YR 2/1) manganese concretions; 2 percent rounded gravel; slightly acid; clear smooth boundary.

Bt—(33 to 74 cm); yellowish brown (10YR 5/6) silty clay; moderate medium angular and subangular blocky structure; friable; slightly sticky, moderately plastic; few very fine and fine, roots; common distinct clay films on faces of peds; many medium prominent light olive brown (2.5Y 5/4) masses of iron accumulation; common medium prominent grayish brown (2.5Y 5/2) iron depletions; common medium and fine prominent black (10YR 2/1) manganese nodules and concretions; 2 percent rounded gravel; strongly acid; clear wavy boundary.

Btg1—(74 to 100 cm); olive gray (5Y 5/2) silty clay; moderate medium angular blocky structure; very firm; very sticky, very plastic; common pressure faces; many prominent clay films on faces of peds; common medium prominent light olive brown (2.5Y 5/4) masses of iron accumulation; common medium prominent black (10YR 2/1) manganese nodules and concretions; 2 percent rounded gravel; mildly alkaline; clear wavy boundary.

Btg2—(100–130 cm); same description as Btg1, but contains calcite films and coatings on ped faces and in very fine root pores, and some evidence for development of pedogenic slickenside surfaces.

Cg—(130 to 183 cm); gray (N 6/) silty clay loam; massive; very firm; very sticky, very plastic; many coarse prominent yellowish brown (10YR 5/6) masses of iron accumulation; common fine prominent black (10YR 2/1) manganese concretions; 5 percent rounded and subrounded gravel; moderately alkaline. (note: 183–270-cm interval was not described in the field)

R—(270 cm) Chickamauga Limestone (Middle Ordovician) — hard, dark black to gray, thinly laminated, micritic limestone.

Latitude: 35°10′21″N; *Longitude*: 85°2′28″W; *UTM Zone*: 16; *Datum*: 1927 North American Datum.

Ketona silty clay loam to silt loam (USDA-NRCS pedon code: S02-TN-065-1)

Ap—(0 to 18 cm); brown (10YR 4/3) silty clay loam; moderate medium granular structure; very friable, slightly sticky, slightly plastic; many fine roots; common medium prominent yellowish red (5YR 5/6) oxidized root channels; few fine prominent black (10YR 2/1) manganese nodules and concretions; <1 percent rounded and subrounded gravel; moderately acid; abrupt smooth boundary.

Btg1—(18 to 51 cm); dark grayish brown (2.5Y 4/2) silty clay loam; moderate medium angular blocky structure; firm, moderately sticky, very plastic; few very fine and fine roots; many distinct clay films on faces of peds; many medium prominent strong brown (7.5YR 4/6) masses of iron accumulation; few fine prominent black (10YR 2/1) manganese nodules and concretions; <1 percent rounded and subrounded gravel; neutral; clear wavy boundary.

Btg2—(51 to 86 cm); dark grayish brown (2.5Y 4/2) silty clay loam; moderate medium angular blocky structure; very firm, moderately sticky; very plastic; very few fine and very fine roots; common pressure faces; many prominent clay films on faces of peds; common medium distinct light olive brown (2.5Y 5/4) masses of iron accumulation; common fine prominent black (10YR 2/1) manganese nodules and concretions; 5 percent rounded and subrounded gravel; neutral; gradual wavy boundary.

Btg3—(86 to 147 cm); grayish brown (2.5Y 5/2) silt loam; weak medium and fine angular blocky structure; very firm, moderately sticky, very plastic; common pressure faces; many prominent clay films on faces of peds; many medium prominent brownish yellow (10YR 6/6) and strong brown (7.5YR5/6) masses of iron accumulation; common prominent black (10YR 2/1) manganese nodules and concretions; 5 percent rounded and subrounded gravel; mildly alkaline; gradual smooth boundary.

BCg—(147 to 170 cm); grayish brown (2.5Y 5/2) silt loam; weak fine and medium angular blocky structure; very firm, moderately sticky, very plastic; common coarse prominent brownish yellow (10YR 6/6) masses of iron accumulation; common medium prominent gray (5YR 5/1) iron depletions; common fine prominent black (10YR 2/1) manganese nodules and concretions; 2 percent rounded and subrounded gravel; mildly alkaline; gradual wavy boundary.

Cg—(170 to 203 cm); gray (N 5/) gravelly loam; massive; very firm, moderately sticky, very plastic; common coarse prominent brownish yellow (10YR 6/6) masses of iron accumulation; common fine and medium prominent black (10YR 2/1) manganese nodules and concretions; 15 percent rounded and subrounded chert gravel; neutral.

After the pit was sampled, the backhoe deepened the excavation in an attempt to find a bedrock contact. The following observations were recorded from backhoe bucket samples: ~274 cm light bluish gray (10B 7/1) extremely gravelly sandy clay loam; many medium light olive brown (2.5Y 5/6) masses of iron accumulation; 65 to 75 percent chert gravel; ~305 cm light bluish gray (10B 7/1), extremely gravelly clay; 65 to 75 percent chert gravel.

R—(315 cm) Chickamauga Limestone (Middle Ordovician) — hard, dark black to gray, thinly laminated, micritic limestone.

Latitude: 35°10′26″N; *Longitude*: 85°2′28″W; *UTM Zone*: 16; *Datum*: 1927 North American Datum.

contact at about 315 cm. A parallel suite of bulk samples, collected by horizon, was sent to the USDA National Soil Survey Laboratory in Lincoln, NE for standard soil characterization (procedures described in Soil Survey Staff (1996)). Oriented thin-section samples were collected from each soil horizon. All thin-section samples were later air-dried, epoxy-impregnated, and then commercially prepared. Micromorphological descriptions primarily follow Fitzpatrick (1993) and Stoops (2003).

After manual removal of macroscale organic matter and oven drying at 60°C, pressed pellets were prepared from bulk, powdered soil samples and analyzed for selected major, minor and trace elements using a Philips wavelength-dispersive X-ray fluorescence (XRF) analyzer (Singer and Janitzky, 1986). The XRF analytical protocol employed appropriate clay soil standards and reports major elements in oxide weight percent and trace elements in ppm (Appendices A and B). Bulk density was determined by paraffin coating of air-dried soil clods (Blake and Hartge, 1986). Particle size and other wet-chemical soil characterization (e.g., pH, Ammonium Acetate-extractable Ca, Dithionate Citrate-extractable Fe, Acid Oxalate-extractable Fe, Total C) were determined at the US Department of Agriculture (USDA), National Soil Survey Laboratory in Lincoln, Nebraska; the laboratory methods for these analyses are described in Soil Survey Staff (1996).

Stable isotope analyses utilized dried soil (~60–200 mg sample to yield ~1 mg of carbon), after reaction with 1N HCl to remove carbonate, which was loaded into a 25-cm-long quartz tube together with 500 mg of CuO, 500 mg of purified granular copper (20–30 mesh) and a 2-cm-long platinum wire. After cooling to air temperature, the quartz tubes were sealed under vacuum, and samples combusted in a muffle furnace at 800°C for 3 h. The CO_2 gas evolved during combustion was collected and cryogenically purified, then analyzed by mass spectrometry (Finnigan Delta Plus

https://doi.org/10.1016/j.yqres.2007.12.003 Published online by Cambridge University Press

Dual-Inlet) at the University of Tennessee. The results are expressed in $\delta^{13}C$ values with respect to the V-PDB standard.

$$\delta^{13}C = \left\{ \left[\left({}^{13}C/{}^{12}C \right)_{sample} / \left({}^{13}C/{}^{12}C \right)_{PDB} \right] - 1 \right\} \times 1000‰$$

Repeated combustion and analysis of USGS-24 graphite standard over the last 20 months during which these samples were analyzed gave a value of −15.998±0.050‰ (n=47) with a measurement standard deviation of 0.0141‰ (n=47), in good agreement with the value of −15.99±0.10‰ reported by Stichler (1995). AMS ^{14}C sample ages for bulk soil organic matter were provided by Beta Analytic, Inc. and are reported here as uncalibrated (raw) radiocarbon dates. Precise locality information is given in Table 1, and bulk density and all geochemical analyses are provided in Appendices A and B.

Results

Morphology

Detailed soil descriptions, based on field observations and supplemented with laboratory data, are included in Table 1. Horizons of the Tupelo pedon (fine, mixed, active, thermic Aquic Hapludalf in USDA Soil Taxonomy) consist of, in descending order from the soil surface: 1) a surface plow layer that is densely rooted by grasses (Ap horizon); 2) an eluviated (BE) horizon slightly enriched in silt

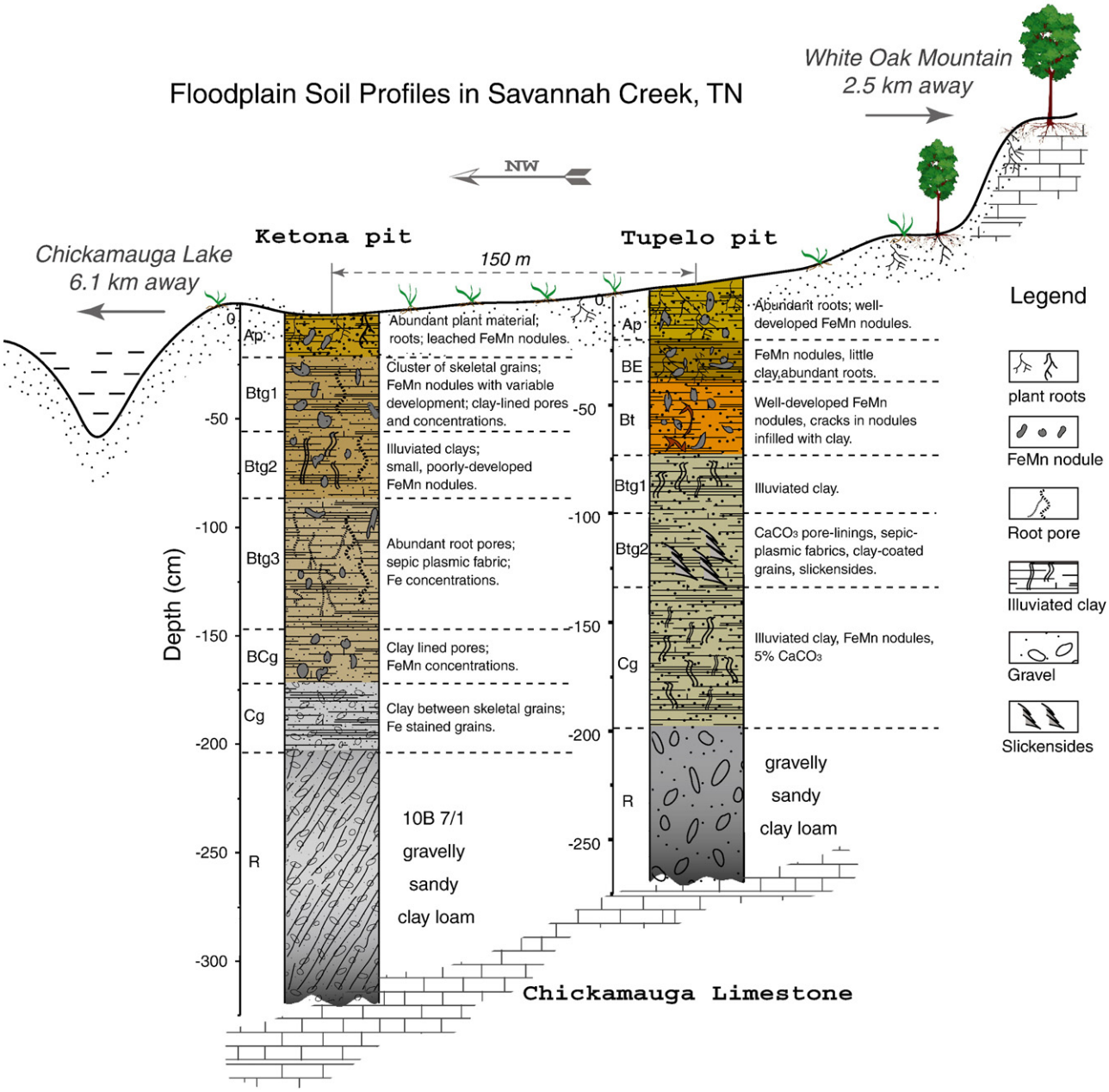

Figure 2. Soil morphologic and micromorphologic descriptions for Tupelo series (fine, mixed, (active), thermic Aquic Hapludalf) and Ketona series (fine, mixed, (active), thermic Typic Epiaqualf) soils from southeastern Tennessee. Horizon designations are shown for each soil (see detailed soil description in Table 1) as well as important micromorphological features (see text for discussion).

https://doi.org/10.1016/j.yqres.2007.12.003 Published online by Cambridge University Press

and sand due to clay removal; 3) a translocated clay-enriched argillic (Bt) horizon that contains illuviated clay and hard Fe concretions; 4) a clay-enriched Btg horizon that has reduced color, Fe-enriched mottles and concretions, as well as portions of soil matrix and macropores depleted in Fe; and 5) a deepest Cg horizon that has less clay than the overlying horizons but has reduced color, mottling, and Fe concentrations as in the overlying horizons (Fig. 2). Chert gravel is locally abundant near the base of the soil profile, which has a sharp boundary with unweathered Chickamauga Limestone (Middle Ordovician) at a depth of 270 cm. The soil matrix is generally leached of calcite except within the 120–140-cm depth interval, where a very weak reaction with HCl occurs. Weakly developed pedogenic slickensides are present within the 100–130-cm depth interval.

Horizons of the Ketona pedon (fine, mixed, active, thermic, Typic Epiaqualf [or Endoaqualf] in USDA Soil Taxonomy) consists of, in descending order from the soil surface: 1) a surface plow layer that is densely rooted by grasses (Ap horizon); 2) a series of stacked horizons enriched in illuviated clay, but showing evidence for redoximorphy, such as Fe-enriched mottles and concretions, as well as portions of soil matrix and macropores depleted in Fe (Btg1, Btg2, Btg3 horizons); 3) a transitional sandy clay (BCg) horizon, and 4) a gravelly loam (Cg) horizon containing abundant chert (Fig. 2). Chert gravel is very abundant near the base of the soil profile, which has a sharp boundary with unweathered Chickamauga Limestone (Middle Ordovician) at a depth of 315 cm. The soil matrix is completely leached of calcite. Fe

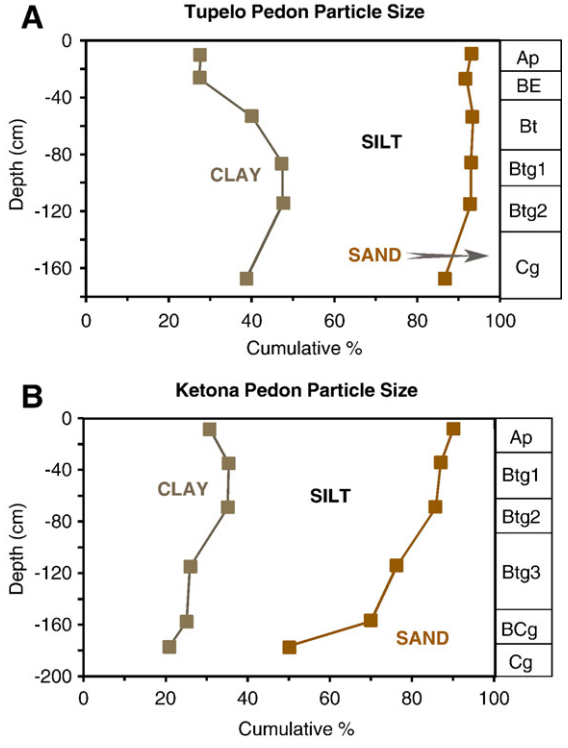

Figure 3. Particle size analysis of Tupelo (A) and Ketona (B) soils, vs. depth. Note stronger development of argillic (Bt) horizons in Tupelo soil based on clay content distribution, and distinct sedimentary fining-upward pattern for Ketona soil based on sand content. Horizons are shown for each soil profile. See text for discussion.

Table 2
Particle size for sand–silt fractions, on a clay-free basis, for Tupelo and Ketona soils

Tupelo S02TN-065-1: fine, mixed, active, thermic Aquic Hapludalf. Note that there is no fining-upward pattern, and that there is some indication of a sediment discontinuity at 130 cm, particularly in fine silt (underline denotes possible sediment break)

Horizon	Depth (cm)		% vcs	% cs	% ms	% fs	% vfs	% csi	% fsi
	Top	Base							
Ap	0	20		tr	1	2	6	20	70
BE	20	33		tr	2	3	6	19	69
Bt	33	74	1	1	1	2	6	23	66
Btg	74	130	1	2	2	3	5	18	69
Cg	130	183	2	3	4	5	8	21	57

Ketona S02TN-065-2: fine, mixed, active, thermic Typic Epiaqualf (Endoaqualf?). Note that there is a distinct fining-upward pattern, with sediment discontinuities (underlined) at 18, 86, 147 and 170 cm

Horizon	Depth (cm)		% vcs	% cs	% ms	% fs	% vfs	% csi	% fsi
	Top	Base							
Ap	0	18	1	1	3	4	5	20	66
Btg1	18	51	2	3	4	4	8	26	54
Btg2	51	86	1	3	6	6	6	21	57
Btg3	86	147	1	2	7	9	13	27	41
BCg	147	170	1	2	11	13	14	27	33
Cg	170	183	4	9	27	13	10	17	20

Vcs = very coarse sand; cs = coarse sand; ms = medium sand; fs = fine sand; vfs = very fine sand; csi = coarse silt; fsi = fine silt.

concretions and mottles extend nearly to the soil surface. Filled crayfish burrows (refilled krotovina in soil science terminology) are common and extend from the soil surface to at least 180-cm depth.

Particle size distribution and parent material uniformity

Textural properties of the soils are summarized in Figure 3 and in Table 2. Whereas the Tupelo profile exhibits a significant increase in clay content with depth, with a major change in particle size distribution occurring at 33 cm within the argillic horizon (Fig. 3A), the Ketona profile, in contrast, has a significant increase in sand content with depth, commencing at 120 cm (Fig. 3B). Clay-free particle size data for sand and silt (Table 2) indicate that the Ketona pedon is overall a fining-upward sequence, which is a common particle-size pattern in proximal alluvial deposits, whereas the Tupelo does not show these characteristics, which likely reflects more distal floodplain conditions (e.g., Aslan and Autin, 1998, 1999). Sediment discontinuities are evident in the Ketona profile at 18, 86, 147, and 170 cm, whereas there is only 1 discontinuity suggested at 130 cm in the Tupelo profile (Table 2).

Plots of wt% Zr vs. Zr/TiO_2 and wt% TiO_2 vs. TiO_2/Zr (e.g., Driese et al., 2000, 2003, 2005) indicate that there is a discontinuity in the Tupelo profile between 120 and 130-cm depth (Figs. 4A, B), which also corresponds to low-chroma color (5Y 5/2) associated with the boundary between the Btg2 and Cg horizons (Table 1; Fig. 2). In particular, upper Tupelo soil material has much higher TiO_2 contents (1.2–1.4 wt%) than lower Tupelo soil (0.85–1.05 wt%), and the three highest Ketona soil samples show a similar characteristically high TiO_2 contents. Zr content, in contrast, does not appear to delineate breaks in parent materials.

https://doi.org/10.1016/j.yqres.2007.12.003 Published online by Cambridge University Press

Micromorphology

Tupelo profile

Tupelo soil micromorphology changes markedly with depth, and these changes are summarized here and in Figure 2. Ap horizon (0–20 cm) silty clay loam contains abundant plant roots and macropores formed from decayed roots (Fig. 5A). Fe/Mn concretions with sharp margins are common and appear as cemented aggregates of quartz silt, clay, and Fe/Mn oxides. Earthworm burrows and castings are common. BE horizon (20–33 cm) silty clay loam contains Fe/Mn concretions with either sharp or diffuse margins (Fig. 5B). Rooting density is less than that in the Ap horizon. Bt horizon (33–74 cm) silty clay contains prominent clay illuviation features, including meniscate clay with high birefringence that infills root macropores and coats ped faces (Fig. 5C). Fe/Mn concretions with sharp margins, numerous growth bands, and engulfing quartz silt and clay are locally abundant. Redox enrichment (dark) and depletion (light) coatings and hypocoatings within old root channels are locally abundant in the Bt horizon and impart a mottled appearance (Fig. 5D). Btg1 horizon (74–100 cm) silty clay contains abundant redox-related features, including redox depletion and enrichment of Fe/Mn in root macropores and other interpedal pores, as well as common Fe/Mn concretions and glaebules with sharp margins (Fig. 5E). The amount of redox-related features is markedly higher than that observed in the Bt horizon. Btg2 horizon (100–130 cm) silty clay has a micromorphology that is similar to that observed in the upper part, but with the addition of fine calcite microspar coating root pores, in which the central pore space is cemented by calcite spar (Fig. 5F); these calcite pore-linings do not occur in any other horizon. Cg horizon (130–186 cm) clay has similar redox-related features as occur in the Btg horizon, but additionally the Cg horizon contains birefringent clays aligned along specific planes, which define stress cutans formed on ped faces and slickensides.

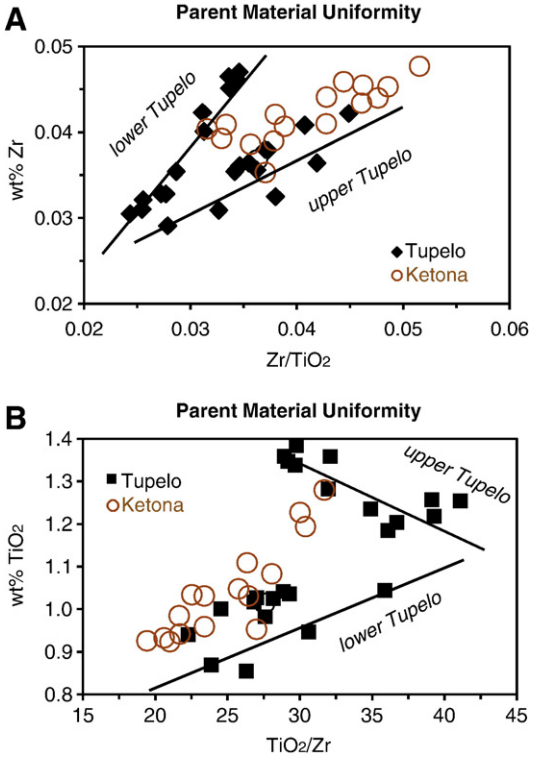

Figure 4. Assessment of parent material uniformity for Tupelo and Ketona soils. (A) Wt% Zr vs. Zr/TiO_2 showing distinctive trends for upper (above 130-cm soil depth) and lower (below 130 cm) Tupelo. (B) Wt% TiO_2 vs. TiO_2/Zr showing distinctive trends for upper and lower Tupelo. Note higher TiO_2 contents of upper Tupelo and for upper 3 samples (circled) of Ketona soil.

Ketona profile

The Ketona soil has a micromorphology dominated by redox-related features summarized here and in Figure 2. Ap horizon (0–18 cm) silty clay loam has abundant root pores, live roots, and worm and insect casts (Fig. 6A). Btg1 horizon (18–51 cm) silty clay loam contains prominent redoximorphic features, including reduced (gley) soil matrices around macropores and fine Fe/Mn nodules engulfing quartz silt and sand grains (Fig. 6B). Btg2 horizon (51–86 cm) silty clay loam has a strongly Fe-depleted (gley) matrix and very abundant, fine to medium Fe/Mn nodules containing engulfed quartz silt and very fine sand (Fig. 6C). Boundaries between Fe/Mn nodules and soil matrix range from sharp to diffuse, and the Btg2 horizon also has root and interpedal macropores coated with illuviated clay (Fig. 6D). Btg3 horizon (86–147 cm) silt loam contains much fewer Fe/Mn nodules, but illuviated clay pore-linings are similar to those observed in the Btg2 horizon (Fig. 6E). BCg horizon (147–170 cm) loam is characterized by a reduced matrix and large macropores infilled with vadose geopetal silt and banded illuviated clay; Fe/Mn occurs as pore-linings and as grain coatings (Fig. 6F). Quartz and chert grains range in size from very fine to coarse sand. Cg horizon (170–183 cm as described) gravelly loam is dominated by angular to subrounded chert sand and gravel grains that exhibit ghost textural features inherited from the limestone precursor, such as ooids and peloidal grains. No grains of unweathered Chickamauga Limestone bedrock occur in the Cg horizon.

Soil characterization data

Selected soil characterization data are summarized in Table 3. Both soil profiles show the general pattern of higher organic C at the soil surface and declining amounts with depth, but complicated by abrupt increases at depth (Btg and Cg horizons in Tupelo, Btg2 horizon in Ketona). Occurrence of low-chroma colors (5Y 5/2) in the Tupelo profile appears to coincide with the increase in organic C and might reflect a buried soil surface. Exchangeable Ca and Mg increase markedly at the Btg horizon in the Tupelo profile and in the Btg1 horizon of the Ketona profile. Free $CaCO_3$ is only present in the Cg horizon of the Tupelo profile. Comparisons of total element data with depth were made between the two soil profiles in order to correlate them geochemically, using both major and minor elements and trace elements (Fig. 7). All geochemical and soil characterization data indicate that the basal 60 cm of soil in the 180 cm Ketona profile are geochemically most like the upper 60 cm of the 240 cm Tupelo profile, as shown in Figure 7, and the offset correlation was consistent for nearly all of the elements examined (see other Appendix A and B data) and has important

https://doi.org/10.1016/j.yqres.2007.12.003 Published online by Cambridge University Press

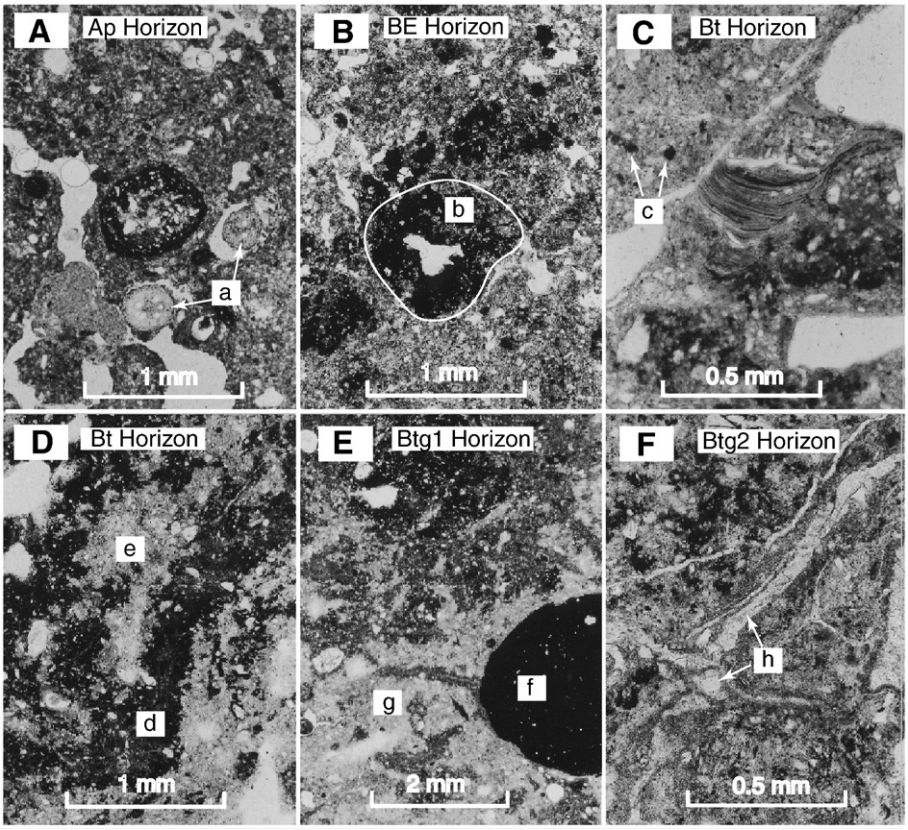

Figure 5. Thin section photomicrographs of Tupelo soil; all photos are plane-polarized light (PPL). (A) Ap horizon (0–20 cm): silty clay loam containing live roots (a) and root pores, and Fe concretion (opaque) containing cemented quartz sand and silt grains. (B) BE horizon (20–33 cm): silty clay loam containing aggrading Fe concretion (b) with hollow center and smaller surrounding concretions. (C) Bt horizon (33–74 cm): silty clay exhibiting root pore partially infilled with illuviated pedogenic clay (meniscate microlaminations); note fine disseminated Fe/Mn oxides/oxyhydroxides in matrix (c). (D) Bt horizon (33–74 cm): silty clay exhibiting redox enrichment (d) and depletion (e) coatings and hypocoatings within old root channels. (E) Btg1 horizon (74–100 cm): silty clay containing large Fe/Mn concretion (f) and surrounding halo of Fe-depleted soil matrix (g). (F) Btg2 horizon (100–130 cm); silty clay containing calcite lining a root pore (h) composed of microspar sheath and central sparry calcite pore-filling.

implications for interpreting both the carbon isotope record and paleoclimate history, as discussed in subsequent sections.

Stable isotope geochemistry and geochronology

Stable carbon isotopes of soil organic matter (SOM) are identical in the Ap and upper Bt/Btg horizons of both profiles, ranging between −24 to −25.5‰. At depths of 100 and 210 cm in the Tupelo profile, and at 80 and 140 cm in the Ketona profile, there are excursions in $\delta^{13}C$ values towards heavier values (maxima of −21.1 and −23.2‰ for the two soils, respectively), and the depth plots of geochemical data suggest that the carbon isotope records overlap by only 60 cm of soil material (Figs. 8, 9). Such a correlation also shows correspondence with radiocarbon dates all appearing in the correct age order (Figs. 8, 9). Calculated fractions of C_3 and C_4 plants contributing to the organic C pool are depicted in Figure 9. The ^{14}C raw chronology (AMS ^{14}C) for bulk humates for the following soil depths are: (1) Tupelo, 130-cm depth (Beta 178624), age=6070±40 ^{14}C yr BP; (2) Tupelo, 240 cm (Beta 178625), 6350±40 ^{14}C yr BP; (3) Ketona, 160 cm (Beta 178622), 5810±40 ^{14}C yr BP; (4) Ketona, 350 cm (Beta 178624), 3530±40 ^{14}C yr BP. The age measured at 350-cm depth in Ketona gravelly clay was rejected as spurious because of its out-of-sequence age and its location along the unconformable boundary between the alluvium and the limestone bedrock, where it was susceptible to contamination from organic matter carried in groundwater.

Interpretations

The two soil profiles, separated by 150-m horizontal distance and differing by only 10 cm in elevation, are interpreted as representing a portion of a floodplain *catena*, whose origin is likely due to differences in seasonal soil hydrology, rather than any significant change in topography (Birkeland, 1999) (Figs. 2, 9). Although both soils are broadly similar in their classification as Alfisols, they differ substantially in terms of their field macromorphology and horizonation, micromorphology, and geochemistry. We will first consider the soil ecosystem, time and parent material correlations that can be established between the two soils. Then, in what follows we interpret the variations in $\delta^{13}C$ values for SOM for the two profiles as indicating high-frequency climate cycles of ~300-yr duration.

Geochronology and allostratigraphy

The results of the ^{14}C AMS dating of the bulk humates indicate that deposition of the alluvial fill of the Savannah Creek Valley probably commenced in the early to mid-Holocene, prior to 5810–6350 ^{14}C yr BP. These dates are consistent with the observed

https://doi.org/10.1016/j.yqres.2007.12.003 Published online by Cambridge University Press

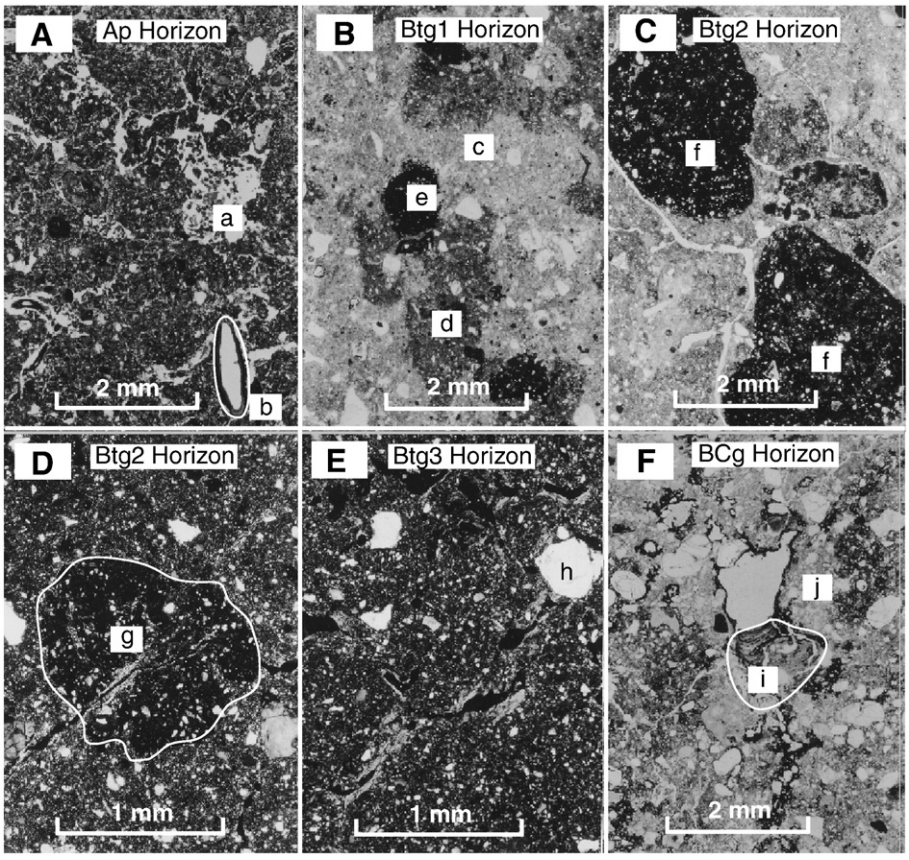

Figure 6. Thin section photomicrographs of Ketona soil; all photos are plane-polarized light (PPL) except for (D) and (E) which are cross-polarized light (XPL). (A) Ap horizon (0–18 cm): silty clay loam containing worm castings (a) and abundant live roots (b). (B) Btg1 horizon (18–51 cm): silty clay loam with prominent redox depletions (c) and enrichments (d), and Fe/Mn concretions (e). (C) Btg2 horizon (51–86 cm): silty clay loam with Fe-depleted matrix and large Fe/Mn concretions (f) containing quartz sand and silt. (D) Btg2 horizon (51–86 cm): clay with cracked Fe/Mn concretion (g) containing birefringent illuviated clay (bright) and included quartz sand and silt. (E) Btg3 horizon (86–147 cm): silt loam with quartz sand grains (h) and fine root or interpedal pores coated with birefringent illuviated clay (bright). (F) BCg horizon (147–170 cm): sandy clay with large macropore partially infilled with geopetal vadose silt (i); note also redox depleted matrix (j) and some Fe/Mn oxides/oxyhydroxides coating grain and macropore surfaces.

degree of soil development (these soils are Alfisols, not Ultisols; e.g., Birkeland, 1999) and the geochronology (older dates under younger dates). There is abundant evidence of localized groundwater flow channeled along the unconformity at the base of the alluvium (e.g., see large macropores in Fig. 6F), and we interpret the spurious younger date reported previously as the result of contamination by younger carbon introduced by water carrying organic C from above. Figures 7 and 8 summarize allostratigraphic and time correlation between the two soil profiles based upon the data presented previously, in which we proposed that the basal 60 cm (soil depth 120–180 cm) of the Ketona soil is time-equivalent to the upper 60–70 cm of the Tupelo soil, and that the upper 120 cm of the Ketona soil formed from alluvium that was deposited after deposition of Tupelo soil material.

Based on the preserved thickness of alluvial sediment and soil material, and estimated durations of deposition ranging from 1000–6000 yr, we determined an average sediment accumulation rate of about 0.5–3 mm/yr. This estimate, of course, does not account for the intermittent nature of sediment accumulation typical of alluvial floodplain surfaces, nor does it account for actual time duration of pedogenesis. As noted previously, the particle size data, on a clay-free basis, suggest possible sediment breaks in the Btg horizon of the Tupelo profile, and in the Ap, Btg2, Btg3 and BCg horizons of the Ketona profile, based upon the fine silt distributions (Table 2). Immobile element data further suggest a major discontinuity in the Tupelo profile at a depth of 130 cm (Btg2/Cg horizon), characterized by a shift from lower to higher TiO_2 content sediments over time (Fig. 4), represented in Figure 8 as lower and upper allostratigraphic units. The offsets in trends of declining organic C with depth, characterized by excursions to higher organic C contents at depth in both the Tupelo and Ketona soils, indicate that there are possible buried A horizons; these were apparently so modified by younger pedogenic processes that they were not initially recognized as such in the field (Tables 1, 3). The low-chroma Btg horizon in the Tupelo profile and the high organic C-content Btg2 horizon in the Ketona soil both likely represent buried A horizons, thus recording periods of non-deposition and pedogenesis on the floodplain surface (Fig. 2; Table 3).

A minimum estimate for duration of pedogenesis, based on the degree of Bt horizon development, would be at least 4000–5000 yr (Birkeland, 1999). Thus the floodplain may have been more depositionally active prior to 6000–7000 yr ago but then became geomorphically stable and subject to pedogenesis during the past 5000–6000 yr. Thus there were at least two previous periods of geomorphic stability and pedogenesis recorded by buried A horizons in the Tupelo and Ketona profiles. However,

https://doi.org/10.1016/j.yqres.2007.12.003 Published online by Cambridge University Press

Table 3
Tupelo and Ketona soil characterization data

Tupelo

Horizon	Depth (cm)	Total C (%)	Soil color	Ext. Ca (meq/100 g)	Ext. Mg (meq/100 g)	$CaCO_3$ (%)
Ap	0–20	1.73	2.5Y 5/3	10.8	0.6	–
BE	20–33	0.91	2.5Y 5/4	9.0	0.4	–
Bt	33–74	0.33	10YR 5/4	7.8	1.6	–
Btg	74–130	0.47	5Y 5/2	21.7	4.2	–
Cg	130–183(+)	0.69	N6/	*	3.5	5

Ketona

Horizon	Depth (cm)	Total C (%)	Soil color	Ext. Ca (meq/100 g)	Ext. Mg (meq/100 g)	$CaCO_3$ (%)
Ap	0–18	2.05	10YR 4/3	12.2	0.9	–
Btg1	18–51	0.47	2.5Y 4/2	16.4	1.5	–
Btg2	51–86	1.02	2.5Y 4/2	15.6	1.0	tr
Btg3	86–147	0.14	2.5Y 5/2	10.4	1.0	tr
BCg	147–170	0.09	2.5Y 5/2	10.3	1.0	tr
Cg	170–183(+)	0.11	N6/	7.9	0.8	tr

* includes Ca from carbonate.

the development of Bt horizons over such a short time seems contradictory with the current wet and poorly drained soil system; this aspect will be addressed in the following section.

Soil drainage history

Both the Tupelo and the Ketona soils currently show abundant field morphological and micromorphological evidence of *redoximorphy*, or Fe and Mn redistributions related to changes in Eh, which are typically caused by seasonal changes in saturation and aeration (Vepraskas, 1992, 2001; Vepraskas et al., 1994) (Fig. 2). Diagnostic features include gray or low chroma (<3) soil colors, soil macropores with Fe/Mn oxide or oxyhydroxide redox depletions and enrichments in the adjacent soil matrix, and Fe/Mn oxide or oxyhydroxide nodules and concretions. Redoximorphic features in soils can record effects of both groundwater fluctuations (*groundwater gley*; known as "endosaturation" in soil science terminology) and stagnation of surface water (*pseudo-gley* of PiPujol and Buurman (1994); "episaturation" in soil science terminology). Aquic moisture regimes occur in soils that are seasonally saturated with groundwater for sufficient periods to cause the soils to be anaerobic (Hurt et al., 1998). Gray or low chroma (<3) colors identify seasonal waterlogging in many soils, except for cases where there are low concentrations of readily oxidizable organic matter (Vepraskas and Wilding, 1983a), or where soil temperatures during the period of saturation are <5°C. To generate soluble Fe there must be a source of at least 1 wt% organic C that can be oxidized in the macropores, a requirement clearly met in both the Tupelo and Ketona profiles (Table 3).

Micromorphological indicators of redoximorphy in the Tupelo and Ketona soils include coatings and nodules formed by the reduction, movement, and oxidation of Fe and Mn within the soil matrix (Figs. 5, 6) (Stoops, 2003). Coatings commonly form along soil macropores such as root channels and ped faces, and are of two general types: (1) *Redox depletion coatings* form adjacent to macropores by movement of Fe and Mn out of the soil matrix (Vepraskas, 1992; Vepraskas and Guertal, 1992 (exemplified in Figs. 5E; 6B, C), and in some cases, by loss of clay (Vepraskas and Wilding, 1983b). (2) *Redox enrichment coatings* form by transport of soluble Fe and Mn, and their reoxidation within the soil matrix in or adjacent to a macropore (Vepraskas, 1992; Vepraskas and Guertal, 1992) (Figs. 5D, F).

However, several relict micromorphological soil features indicate a previous history for these floodplain soils that included

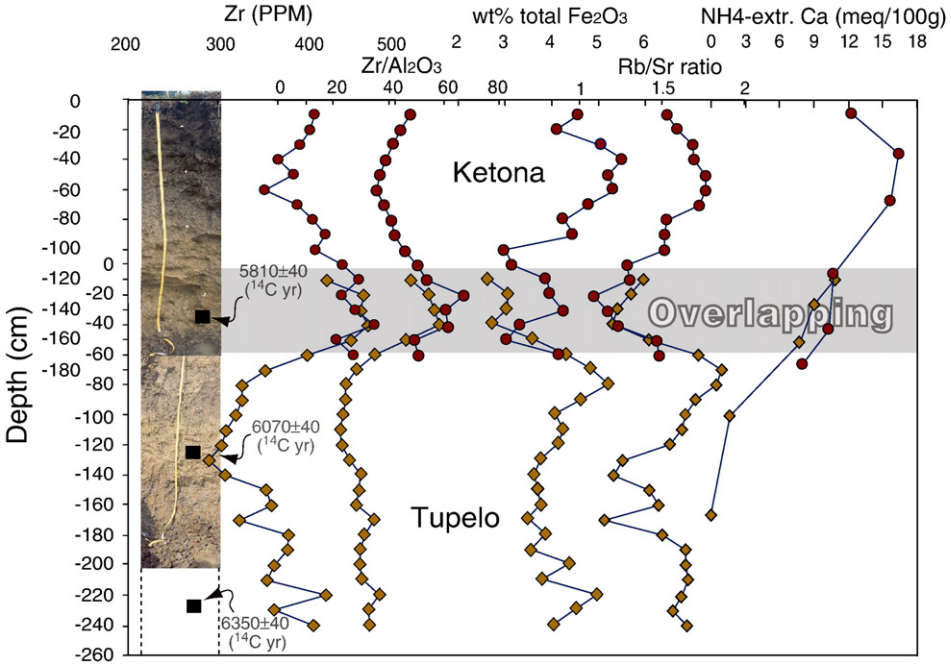

Figure 7. Zr (ppm), Zr/Al_2O_3, wt% Fe_2O_3, Rb/Sr (all measured using XRF on whole-soil), and NH_4-extractable Ca (meq/100 g) versus depth, for Tupelo and Ketona soils. Multiple geochemical proxies suggest tentative correlation of surface of Tupelo soil with Ketona soil at 110-cm depth, resulting in 60-cm overlap between two soil profiles (see interpretations presented in Fig. 8). AMS ^{14}C uncalibrated ages from bulk humates are shown (see text for discussion).

https://doi.org/10.1016/j.yqres.2007.12.003 Published online by Cambridge University Press

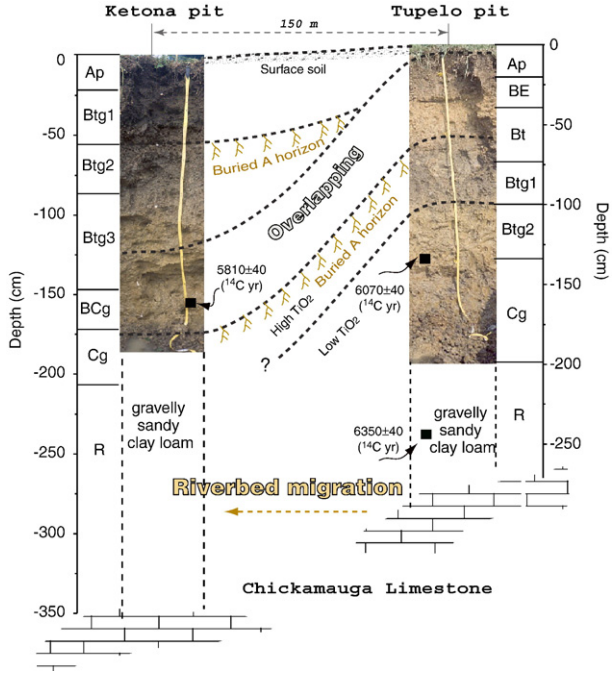

Figure 8. Interpreted allostratigraphy and proposed correlation between two soil pits for alluvium deposited on irregular limestone bedrock surface, and corresponding paleoenvironmental and geomorphic conditions. Tupelo soil is slightly topographically higher and somewhat better drained, but with higher clay content because of distal position from active channel of the two soil sites. Elevated total organic C values at depth point to occurrences of buried A horizons in both soil profiles (e.g., Btg1 horizon of Tupelo soil is a buried soil surface), with 60 cm of overlapping soil/sediment record as shown. Ketona soil is more poorly drained due to lower topographic position, but has distinct higher sand content and fining-upward textural pattern inherited from proximity to active fluvial channel. Note that lower Tupelo soil profile is divisible into upper high-TiO_2 and lower low-TiO_2 successions (see also Fig. 4). AMS ^{14}C uncalibrated ages from bulk humates shown are consistent with this interpreted stratigraphy (see text for discussion).

active clay shrinking and swelling under a drier climate regime, along with better (as compared with current conditions) soil drainage, consistent with postulated mid-Holocene Hypsithermal climate. Pedogenic slickensides were observed in the field in the Btg2 horizon of the Tupelo soil and indicate conditions in which swelling pressures exceeded soil confining pressures, and lateral soil movement occurred along slickenside surfaces (Wilding and Tessier, 1988) (Fig. 2; Table 1). Vadose silt illuviation (translocation) fabrics are present in the BCg horizon of the Ketona profile as well as in the Bt horizon of the Tupelo profile (Figs. 5C; 6F), which indicate the existence of freely-drained (vadose zone) conditions during pedogenesis, when silt grains were transported by soil water into macropores (Brewer, 1976; Bullock et al., 1985; Fitzpatrick, 1993; Stoops, 2003). Illuviated clay exhibiting high birefringence and bright interference colors under cross-polarized light similarly attests to clays carried by soil water under freely drained conditions and deposited on surfaces within macropores (Figs. 5C; 6D, E).

Soils that develop in environments in which precipitation (or soil-moisture deficit) is seasonally variable and that contain expandable clays develop distinctive micromorphologic features related to shrinking and swelling of clays, especially sepic-plasmic (oriented bright-clay) microfabrics characterized by flecked domains of oriented clays arranged in distinctive patterns (Brewer, 1976; Wilding and Tessier, 1988; Blokhuis et al., 1990; Fitzpatrick, 1993). These features were generally present (though weakly expressed; compare with micromorphology of well-developed Vertisols in Driese et al. 2000, 2003; Nordt et al., 2004) in the soils examined in this study. Because pedogenic carbonate precipitation requires some period of aeration and free soil drainage, the presence of pedogenic carbonate in the Btg2 horizon as thin pore-linings and coatings is also not consistent with the current poorly drained soil conditions (Fig. 5F), (Bullock et al., 1985; Fitzpatrick, 1993). Thus, these contradictory micromorphologic features suggest that the Tupelo and Ketona soils must have experienced drier and better-drained times in the past, possibly associated with climate changes affecting the floodplain. The stable isotope record of such postulated drier periods is explored in the following section.

Stable carbon isotopes and soil ecosystems

Many authors have demonstrated that the stable carbon isotopic composition of soil organic matter (SOM) directly records contributions of the soil ecosystem to the soil carbon pool and can therefore track changes in paleoclimate (e.g., Nordt et al., 1994, 2002; Boutton et al., 1993; Cerling and Ehleringer, 2000). C_3 (Calvin cycle) plants produce isotopically more depleted carbon ($\delta^{13}C$ values of SOM average −26‰ PDB) than do C_4 (Hatch–Slack cycle) plants ($\delta^{13}C$ values of SOM average −12‰ PDB). The $\delta^{13}C$ values of soil organic matter (SOM) reflect CO_2 derived from decomposed plant debris over time and are generally good indicators of the average C_3/C_4 plant mix within an ecosystem (e.g., Wang et al., 2000a,b). The C_3 plants include most trees, shrubs and cool-season grasses, whereas C_4 plants are dominantly warm-season grasses, which are better adapted to lower moisture, higher temperatures, and more direct sunlight conditions. Through the use of a simple mixing equation calculated as $\delta^{13}C = -26(X) + -12(1-X)$, where X = fraction of vegetation that utilizes the C_3 photosynthetic pathway, the proportion of C_3/C_4 plants in the soil ecosystem can be estimated (Fig. 9). The $\delta^{13}C$ values of the Tupelo profile at 210-cm depth suggest 65% C_3 and 35% C_4 plants, whereas the least-negative $\delta^{13}C$ values of the Ketona profile at 140-cm depth suggest 80% C_3 and 20% C_4 plants. This difference in ranges of isotopic shifts (greater in Tupelo than for Ketona) might reflect maintenance of generally wetter (or cooler) conditions in the Ketona soil, even during a time of overall drier (or warmer) conditions, because of its lower elevation (and associated water ponding) and closer proximity to the active fluvial channel. An alternative interpretation would be that the ecosystem remained dominantly C_3 composition, but experienced stress due to changes in temperature or water use efficiency manifested by less negative $\delta^{13}C$ values of SOM.

Alteration of SOM by soil microbial processes is a valid concern and might also be a plausible explanation for the shifts in $\delta^{13}C$ values for the two profiles. Many taphonomic, microbial, and diagenetic processes can affect the isotopic composition of terrestrial organic matter prior to its preservation within the geologic record (e.g., Boutton, 1996; Accoe et al., 2002; Johnson et al., 2007). In a soil system, surface-derived organic matter is mixed into deeper soil layers by bioturbation by plant roots and animals, or may be translocated by soil water moving through macropores, after which it is metabolized by soil microbes. An alternative hypothesis might therefore consider the possibility that

https://doi.org/10.1016/j.yqres.2007.12.003 Published online by Cambridge University Press

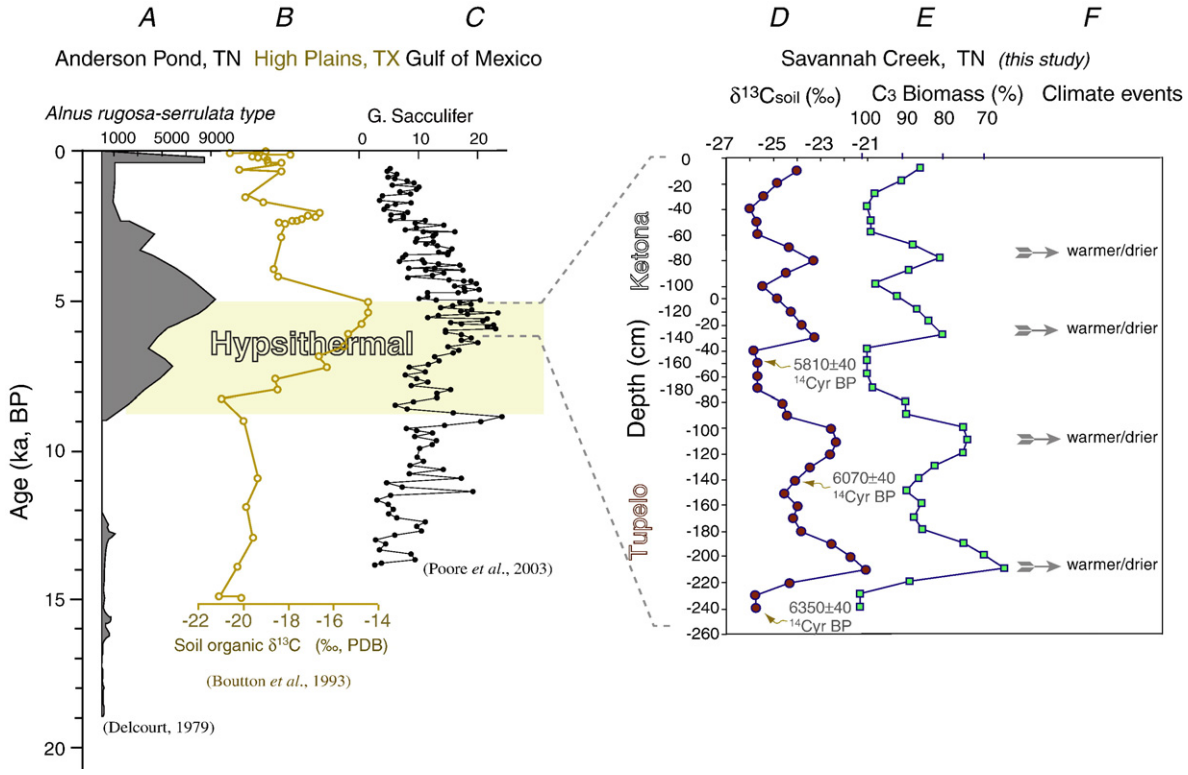

Figure 9. Late Pleistocene to Holocene paleoclimate records from adjacent areas in US and Gulf of Mexico, including: (A) pollen record from Anderson Pond, TN lacustrine deposits (Delcourt, 1979), (B) $\delta^{13}C$ values of SOM in soils and paleosols of High Plains and central TX (Boutton et al., 1993), and (C) abundance of planktonic foraminifera in northern Gulf of Mexico (Poore et al., 2003), compared with (D) $\delta^{13}C$ values of SOM from Tupelo and Ketona soils in southeastern TN, assuming that upper 100–125 cm of Ketona soil is apparently younger than Tupelo soil, and lower 60 cm of Ketona soil pit is correlative with upper 60 cm of Tupelo soil pit (see basis for correlations in Figs. 7 and 8), (E) calculated % C_3 biomass (see text for explanation, and (F) interpreted high-frequency climate shifts to warmer/drier conditions. We interpret the 4 distinct excursions in $\delta^{13}C$ values of 2–4‰ in (D) as evidence for 4 climate changes of ~300-yr duration to warmer and drier conditions during mid-Holocene; the 2–4‰ isotope excursions towards heavier values suggest greater contributions of C_4 plants to the organic C pool (or water stress of C_3 plants) during this time, tentatively correlated with the mid-Holocene warming and drying "Hypsithermal Event" documented elsewhere in North America.

the observed vertical trends in $\delta^{13}C$ values with depth reflect isotopic discrimination against ^{13}C during organic matter decomposition, combined with increasing degree of transformation of organic matter with depth in the soil column. In this case the remaining SOM would assume less negative $\delta^{13}C$ values due to selective removal of ^{12}C. In contrast, in a study of the evolution of organic C content and δ^{13} C values of soil organic matter in a grassland, Accoe et al. (2002) demonstrated that some decomposing organisms actually prefer ^{13}C-depleted molecules for respiration, while the remaining ^{13}C-enriched molecules are used in the production of biomass and the end products of metabolism; this microbial respiration process resulted in a 4‰ shift from the soil surface (−30‰) to −26‰ at a depth of 30 cm, with a corresponding change in organic matter content, from 3.5% at the surface to 0.5% at a depth of 35 cm.

In a recent study by Johnson et al. (2007) of modern soils and Quaternary paleosols in the tallgrass prairie of Kansas, these authors also observed a 3.4‰ ^{13}C depletion in SOM sampled in the upper 20 cm of the soils, and ascribed it to stratification of C_3 and C_4 rooting systems (i.e., C_3 grass roots are shallower than C_4). Interestingly, Johnson et al. (2007) also measured a 2‰ decrease from C_4 grass tissue to the underlying maximum SOM $\delta^{13}C$ values, but could not unequivocally explain the process by which this occurred. With the available data we cannot rule out that either (or both) of these microbial processes, or rooting depth differences between C_4 and C_3 plants, might have affected the stable carbon isotopic composition of the SOM in the Tupelo and Ketona soil profiles. Nevertheless, it is hard to explain the repeated occurrences of (4) cyclical variations in $\delta^{13}C$ values of soil organic matter with depth (Fig. 9), or the occurrences of micromorphological features such as slickensides, sepic-plasmic microfabrics, and carbonate pore-linings (Fig. 2) in association with less negative $\delta^{13}C$ values for SOM, except as indicators of ecosystem (and by inference, climate) change.

Studies of SOM in central Texas and the southern Plains reveal a pattern of increased $\delta^{13}C$ values in the mid-Holocene, indicating more relative C_4 productivity compared to the early Holocene (50–70% C_4; $\delta^{13}C$ values of −20.5 to −17‰ PDB); this event is the well-known Altithermal of the North American Great Plains (Meltzer, 1999; Nordt et al., 1994, 2002). The 2.5–4‰ excursions toward less negative $\delta^{13}C$ values of SOM measured in the Tupelo and Ketona profiles, although not of the magnitude recorded in Texas, perhaps record the same general episode of drier mid-Holocene climate conditions, and this hypothesis is supported by the uncalibrated AMS radiocarbon ages for bulk soil humates reported previously (Figs. 8, 9). But the character of the stable isotope record from the floodplain soils and sediments from southeastern Tennessee is different from that of the Altithermal in that the TN record appears as 4 transient events of relatively short duration, as is discussed in the following section.

https://doi.org/10.1016/j.yqres.2007.12.003 Published online by Cambridge University Press

Discussion

Recent studies of adjacent areas, such as the Gulf of Mexico and Florida Keys, point to millennial- to century-scale climate variability during the past 14,000 yr, including the Little Ice Age and Medieval Warm Period (Lund and Curry, 2004; Poore et al., 2004; Richey et al., 2007). Whether or not there were terrestrial "footprints" of century- to millennial-scale climate oscillations during the mid-Holocene Hypsithermal has not been previously investigated in the southern Appalachian region, where the mountainous terrain is affected by the interplay of two major moisture sources (Gulf of Mexico and Atlantic Ocean). Research by Poore et al. (2003) on planktonic foraminifera in the Gulf of Mexico has documented the occurrences of distinct 300-yr cycles in *G. sacculifer* abundance. Our SOM $\delta^{13}C$ values, supported by micromorphological evidence present within high-sedimentation-rate floodplain deposits from southeastern Tennessee, possibly represent a "terrestrial footprint" for warming and increased aridity during the period ~6500 to 5000 ^{14}C yr BP with ~300-yr cycles (Fig. 9). Interestingly, ^{14}C-dated floodplain profiles from different locations in the southern Appalachian region indicate a cluster development of floodplains starting at about 6400 ^{14}C yr BP (W. Kocis, unpub. data), suggesting early Holocene wet conditions. Our study of a single small floodplain from the southern Appalachian region suggests that the mid-Holocene Hypsithermal was an episodic feature with multiple events. The multiple mid-Holocene warming/drying episodes that we document here are of the same magnitude as the ~400 and ~200-yr cycles reported by Yu and Ito (1999) from a 2100-yr record from a closed-basin lake in the northern Great Plains, which they ascribed to solar (sunspot) forcing; similarly, Wang et al. (2000a,b) reported ~450-yr climate oscillations in a late Wisconsinan loess–paleosol record in the central US, which they interpreted as the result of long-term ENSO cycles. Only one or two phases of mid-Holocene warming are inferred for the southwestern inland region of Texas (Boutton et al., 1993; Nordt et al., 1994), and it is apparent from studies in the Great Plains (summarized in Meltzer, 1999) that it was not hot and dry everywhere during the middle Holocene and at all times; thus, there was much climatic variability. The Hypsithermal has potential as an analog for near-future climate conditions expected in response to present-day global warming, and so a greater understanding of the paleohydrological and paleoclimate impacts on this previously unstudied southern Appalachian region during this time period would be of great value to both climate modelers and governmental agencies.

Our study also demonstrates the importance of higher-resolution (i.e., 10-cm depth interval) sampling of soils and associated floodplain sediments, in contrast to the typical one sample per horizon of most pedological studies. Were the sampling interval not this fine in our study, several major and paleoclimatically significant isotope excursions indicating a soil ecosystem shift in response to a shift to drier climate conditions in the mid-Holocene would not have been detected (Figs. 7, 8, 9). Likewise, our higher-resolution sampling permitted geochemical correlations of parent material using depth variations in Zr and other elements measured in whole-soil samples (Figs. 7, 8). The use of geochemical proxies for correlation, in addition to conventional studies of paleosol morphology and micromorphology, offers exceptional promise in reconstructing paleoclimates in the geologic record.

Conclusions

Two Alfisols developed on an alluvial floodplain in southeastern Tennessee comprise a catena developed due to differences in soil drainage. The soils are spaced 150 m apart, with an elevation difference of only 10 cm, and developed in mid-Holocene alluvium (based on AMS ^{14}C dating of bulk soil humates). The stable carbon isotopic record for soil organic matter, with $\delta^{13}C$ values ranging between −21.1‰ and −26.0‰ PDB, reflects either incursions of some C_4 plants during drier climate phases, or the predominance of C_3 plants but with significant differences in temperature or water use efficiency. These postulated middle Holocene high-frequency climate changes, with possibly 4 drying/warming events of ~300-yr duration, are consistent with Gulf of Mexico paleoclimate records based on foraminifera (Poore et al., 2003) and are tentatively correlated with the mid-Holocene Hypsithermal event. Although redoximorphic processes related to seasonal saturation dominate both soils today, there are abundant relict features (slickensides, vadose silt, illuviated clay, pedogenic carbonate) which developed when the soils were better-drained that also record transient drier conditions present during past times.

This study demonstrates that soils formed on alluvial floodplains are useful for reconstructing paleoclimate, but in order to "read" the floodplain record one must look for not only differences in soil (and paleosol) morphology and micromorphology, but also differences in geochemistry that may only be detectable using closely spaced sampling not traditional for pedologic studies. Floodplains in the southeastern US and other parts of the world have great potential for reconstructing Pleistocene–Holocene climate that is only beginning to be realized.

Acknowledgments

The University of Tennessee (UT) Center for Environmental Biotechnology and the UT Institute for a Secure and Sustainable Environment (formerly the UT Waste Management Research and Education Institute) generously supported this research. We gratefully acknowledge the USDA-NRCS, and especially soil scientist Richard L. Livingston for his assistance with site selection, field sampling and descriptions, and we especially thank Dr. Warren C. Lynn for generously providing soil characterization data through the National Soil Survey Laboratory in Lincoln, NE. We also appreciate the helpful field assistance of Dr. Cynthia Stiles (Wisconsin-Madison). Dr. Lee C. Nordt (Baylor University) kindly reviewed an earlier draft of this manuscript and provided helpful comments. Comments from *QR* Associate Editor Dr. Vance Holliday and two anonymous reviewers greatly approved the quality of the revised manuscript.

Appendix A
X-ray fluorescence geochemical data for Tupelo soil

Sample depth	Sum of conc.	Al_2O_3	Ba	CaO	Cu	Fe_2O_3	K_2O	MgO	Na_2O	P_2O_5	Rb	S	SiO_2	Sr	TiO_2	Zr	Zn	MnO	Y	Co	Cr	V	Hf
		Al	Ba	Ca	Cu	Fe	K	Mg	Na	P	Rb	S	Si	Sr	Ti	Zr	Zn	Mn	Y	Co	Cr	V	Hf
(cm)	(%)	(%)	(ppm)	(%)	(ppm)	(%)	(%)	(%)	(%)	(%)	(ppm)	(ppm)	(%)	(ppm)	(%)	(ppm)	(ppm)	(%)	(ppm)	(ppm)	(ppm)	(ppm)	(ppm)
TUP-10	94.66	8.84	286	0.69	24	2.65	1.14	0.61	0.32	0.146	74	267	78.60	53	1.36	423	49	0.173	37	50	129	36	12
TUP-20	98.38	8.52	284	0.68	24	3.08	1.07	0.58	0.33	0.115	71	124	82.31	54	1.38	465	43	0.183	39	21	131	27	13
TUP-30	98.11	8.18	246	0.65	24	3.04	0.97	0.56	0.34	0.104	67	84	82.68	54	1.35	462	38	0.133	38	21	123	20	12
TUP-40	98.50	8.07	260	0.56	18	2.73	0.92	0.55	0.36	0.092	64	21	83.69	53	1.36	470	35	0.069	37	14	131	14	14
TUP-50	98.18	9.75	264	0.52	23	3.58	1.11	0.66	0.37	0.078	80	15	80.59	56	1.34	451	40	0.071	34	12	130	32	13
TUP-60	96.44	11.51	280	0.56	24	4.33	1.26	0.80	0.34	0.076	100	24	76.14	58	1.28	401	51	0.039	35	16	122	49	12
TUP-70	94.96	12.52	331	0.63	20	4.84	1.33	0.87	0.32	0.077	110	46	72.86	59	1.24	354	55	0.159	39	20	124	50	11
TUP-80	93.85	13.47	457	0.81	21	5.22	1.43	0.98	0.30	0.074	121	85	69.87	66	1.20	328	61	0.357	50	19	124	61	9
TUP-90	94.39	13.45	490	0.91	23	4.64	1.39	1.03	0.31	0.069	123	16	71.06	72	1.18	328	62	0.208	45	15	117	69	9
TUP-100	94.85	13.71	445	0.93	18	4.05	1.31	1.04	0.29	0.066	122	16	71.94	74	1.26	321	60	0.127	41	13	126	61	10
TUP-110	93.54	13.96	445	0.95	18	4.24	1.32	1.06	0.28	0.064	122	36	70.17	75	1.22	310	63	0.147	40	12	123	58	10
TUP-120	94.61	13.40	391	1.15	20	4.15	1.31	1.03	0.32	0.066	117	2	71.74	75	1.25	305	64	0.072	37	12	125	60	9
TUP-130	87.85	11.24	364	6.35	23	3.75	1.20	0.92	0.27	0.061	95	53	62.81	75	1.04	291	54	0.09	39	32	90	56	9
TUP-140	88.06	10.35	337	7.37	19	3.60	1.15	0.85	0.29	0.06	85	88	63.28	70	0.95	309	48	0.052	37	15	91	50	9
TUP-150	94.98	12.19	371	1.02	21	3.69	1.31	0.96	0.36	0.061	93	12	74.20	65	1.04	355	58	0.047	34	15	113	44	12
TUP-160	95.79	12.83	371	0.95	21	3.77	1.36	1.01	0.36	0.065	98	14	74.24	66	1.04	361	64	0.047	34	11	116	52	10
TUP-170	85.24	9.37	299	9.69	21	3.49	1.10	0.77	0.30	0.061	79	9	59.44	68	0.86	325	52	0.05	44	14	79	44	8
TUP-180	94.61	12.22	364	0.99	21	3.87	1.38	0.97	0.37	0.069	98	2	73.50	65	1.03	380	66	0.088	35	16	115	55	11
TUP-190	94.45	12.73	347	1.05	24	3.55	1.45	1.00	0.38	0.066	107	9	73.01	65	1.02	379	63	0.056	35	17	111	55	11
TUP-200	93.12	12.42	390	1.81	23	4.39	1.48	0.96	0.36	0.067	109	37	70.34	66	1.03	364	61	0.149	41	38	112	63	11
TUP-210	90.70	11.71	356	4.31	24	3.80	1.42	0.92	0.34	0.067	110	12	66.98	66	0.98	356	57	0.062	41	18	95	54	8
TUP-220	94.71	11.53	513	1.05	23	4.95	1.43	0.90	0.37	0.079	96	28	73.08	59	0.94	422	52	0.242	37	20	111	66	11
TUP-230	95.49	11.15	349	0.94	25	4.50	1.30	0.85	0.34	0.081	88	42	75.22	56	0.87	364	46	0.108	33	18	106	61	10
TUP-240	95.37	12.34	331	1.02	24	4.03	1.46	0.92	0.35	0.075	98	5	73.98	59	1.00	408	51	0.06	35	16	105	61	12

Appendix B
X-ray fluorescence geochemical data for Ketona soil

Sample depth	Sum of conc.	Al_2O_3	Ba	CaO	Cu	Fe_2O_3	K_2O	MgO	Na_2O	P_2O_5	Rb	S	SiO_2	Sr	TiO_2	Zr	Zn	MnO	Y	Co	Cr	V	Hf
		Al	Ba	Ca	Cu	Fe	K	Mg	Na	P	Rb	S	Si	Sr	Ti	Zr	Zn	Mn	Y	Co	Cr	V	Hf
(cm)	(%)	(%)	(ppm)	(%)	(ppm)	(%)	(%)	(%)	(%)	(%)	(ppm)	(ppm)	(%)	(ppm)	(%)	(ppm)	(ppm)	(%)	(ppm)	(ppm)	(ppm)	(ppm)	(ppm)
KET-10	96.89	8.56	309	0.72	24	3.93	0.96	0.60	0.25	0.141	75	258	80.19	49	1.23	409	49	0.163	35	13	126	71	12
KET-20	97.79	9.15	303	0.75	24	3.59	1.05	0.64	0.25	0.114	83	212	80.68	52	1.28	404	47	0.154	36	10	127	68	12
KET-30	97.54	9.42	339	0.80	25	4.27	1.06	0.66	0.27	0.116	88	174	79.45	52	1.19	393	48	0.164	37	12	123	74	11
KET-40	97.73	9.44	342	0.84	22	4.64	1.08	0.70	0.28	0.100	90	130	79.30	53	1.01	368	47	0.201	35	13	114	77	12
KET-50	97.39	10.50	376	0.83	20	4.40	1.23	0.77	0.29	0.078	97	80	77.91	55	1.08	386	48	0.165	38	10	118	63	11
KET-60	96.88	9.89	352	0.79	25	4.51	1.14	0.73	0.27	0.081	90	42	78.22	51	0.95	353	46	0.170	34	14	105	92	9
KET-70	96.89	10.19	344	0.81	20	4.09	1.14	0.73	0.29	0.071	90	33	78.27	52	1.03	390	45	0.155	36	16	110	81	11
KET-80	96.25	9.89	326	0.78	28	3.71	1.01	0.70	0.29	0.067	78	41	78.55	51	1.05	407	40	0.088	35	13	114	84	10
KET-90	96.86	9.98	330	0.79	22	3.87	1.05	0.70	0.32	0.074	79	32	78.73	52	1.11	421	41	0.130	35	14	119	63	11
KET-100	95.12	9.04	299	0.75	21	2.75	1.00	0.67	0.30	0.076	73	76	79.41	48	0.96	410	38	0.052	32	12	112	80	13
KET-110	98.64	8.70	263	0.69	22	2.87	0.91	0.61	0.31	0.063	62	17	83.33	48	1.03	441	32	0.027	30	17	107	74	13
KET-120	98.62	8.54	293	0.67	23	3.42	0.95	0.60	0.32	0.062	64	3	82.84	49	1.03	459	31	0.062	32	16	108	74	13
KET-130	99.78	6.53	237	0.60	20	3.47	0.80	0.46	0.33	0.072	48	8	86.46	44	0.92	440	23	0.023	29	20	110	73	12
KET-140	97.11	7.51	273	0.64	21	3.67	0.93	0.52	0.36	0.067	54	34	82.28	46	0.99	455	27	0.049	30	31	113	59	13
KET-150	97.90	7.74	254	0.64	25	2.99	0.97	0.55	0.38	0.064	57	5	83.53	46	0.93	477	26	0.009	27	22	105	66	13
KET-160	97.14	8.82	310	0.71	24	2.78	1.08	0.66	0.35	0.072	72	4	81.61	49	0.94	434	37	0.009	33	20	102	69	13
KET-170	96.72	8.93	357	0.72	22	3.60	1.12	0.67	0.36	0.071	73	16	79.96	49	0.93	453	40	0.231	33	22	104	84	12

References

Accoe, F., Boeckx, P., Van Cleemput, O., Hofman, G., Zhang, Y., Li, R.-H., Guanxiong, C., 2002. Evolution of the $\delta^{13}C$ signature related to total carbon contents and carbon decomposition rate constants in a soil profile under grassland. Rapid Communications in Mass Spectrometry 16, 2184–2189.

Aslan, A., Autin, W.J., 1998. Holocene flood-plain soil formation in the southern lower Mississippi Valley: implications for interpreting alluvial paleosols. Geological Society of America Bulletin 110, 433–449.

Aslan, A., Autin, W.J., 1999. Evolution of the Holocene Mississippi River floodplain, Ferriday, Louisiana: insights on the origin of fine-grained floodplains. Journal of Sediementary Research 69, 800–815.

Birkeland, P.W., 1999. Topography—soil relations with time in different climatic settings, Soils and Geomorphology, 3rd ed. Oxford University Press, New York, pp. 230–267.

Blake, G.R., Hartge, K.H., 1986. Bulk density, In: Klute, A. (Ed.), 2nd ed. Methods of Soil Analysis, Part I. Physical and Mineralogical Methods. Soil Science Society of America Agronomy Monograph, vol. 9. Soil Science Society of America, Madison, WI, pp. 363–375.

Blokhuis, W.A., Kooistra, M.J., Wilding, L.P., 1990. Micromorphology of cracking clayey soils (Vertisols). In: Douglas, L.A. (Ed.), Soil Micromorphology: a Basic and Applied Science. Developments in Soil Science, 19. Elsevier Pub. Co., New York, pp. 123–148.

Boutton, T.W., 1996. Stable carbon isotope ratios of soil organic matter and their use as indicators of vegetation and climate change. In: Boutton, T.W., Yamasaki, S. (Eds.), Mass Spectrometry of Soils. Dekker, New York, pp. 47–82.

Boutton, T.W., Nordt, L.C., Archer, S.R., Midwood, A.J., Casar, I., 1993. Stable carbon isotope ratios of soil organic matter and their potential use as indicators of paleoclimate. Isotope Techniques in the Study of Past and Current Environmental Changes in the Hydrosphere and the Atmosphere. International Atomic Energy Agency, Vienna 445–459.

Brewer, R., 1976. Fabric and Mineral Analysis of Soils, 2nd edition. Krieger Pub. Co., New York.

Bullock, P., Fédoroff, N., Jungerius, A., Stoops, G., Tursina, T., 1985. Handbook of Soil Thin Section Description. Waine Research Publications, Albrighton, UK.

Cerling, T.E., Ehleringer, J.L., 2000. Welcome to the C_4 world. In: Gastaldo, R.A., DiMichele, W.A. (Eds.), Phanerozoic Terrestrial Ecosystems, A Short Course. The Paleontological Society Papers, 6. The Paleontological Society, New Haven, CT, pp. 273–286.

Delcourt, H.R., 1979. Late Quaternary vegetation history of the eastern Highland Rim and adjacent Cumberland Plateau of Tennessee. Ecological Monographs 49, 255–280.

Driese, S.G., Mora, C.I., Stiles, C.A., Joeckel, R.M., Nordt, L.C., 2000. Mass-balance reconstruction of a modern Vertisol: implications for interpreting the geochemistry and burial alteration of paleo-Vertisols. Geoderma 95, 179–204.

Driese, S.G., Jacobs, J.R., Nordt, L.C., 2003. Comparison of modern and ancient Vertisols developed on limestone in terms of their geochemistry and parent material. Sedimentary Geology 157, 49–69.

Driese, S.G., Li, Z.-H., Horn, S.P., 2005. Late Pleistocene to Holocene paleoclimate and paleogeomorphic history interpreted from 23,000 ^{14}C yr B.P. paleosol and floodplain soils, southeastern West Virginia, USA. Quaternary Research 63, 136–149.

Dwyer, T.R., Mullins, H.T., Good, S.C., 1996. Paleoclimatic implications of Holocene lake-level fluctuations, Owasco Lake, New York. Geology 24, 519–522.

Fitzpatrick, E.A., 1993. Soil Microscopy and Micromorphology. New York, John Wiley and Sons.

Goman, M., Leigh, D.S., 2004. Wet early to middle Holocene conditions on the upper Coastal Plain of North Carolina, USA. Quaternary Research 61, 256–264.

Harrison, S.P., Kutzbach, J.E., Liu, Z., Bartlein, P.J., Otto-Bliesner, B., Muhs, D., Prentice, I.C., Thompson, R.S., 2003. Mid-Holocene climates of the Americas: a dynamical response to changed seasonality. Climate Dynamics 20, 663–688.

Hurt, G.W., Whited, P.M., Pringle, R.F. (Eds.), 1998. Field Indicators of Hydric Soils in the United States. Natural Resources Conservation Service, Version 4.0. US Department of Agriculture.

Jackson, B.W., 1982. Soil Survey of Hamilton County, Tennessee. U.S. Department of Agriculture, Natural Resources Conservation Service.

Johnson, W.C., Willey, K.L., Macpherson, G.L., 2007. Carbon isotope variation in modern soils of the tallgrass prairie: analogues for the interpretation of isotopic records derived from paleosols. Quaternary International 162–163, 3–20.

Leigh, D.S., Feeney, T.P., 1995. Paleochannels indicating wet climate and lack of response to lower sea level, southeast Georgia. Geology 23, 687–690.

Lund, S., Curry, W.B., 2004. Late Holocene variability in Florida Current surface density: patterns and possible causes. Paleoceanography 19 (4) PA4001. doi: 10.1029/2004PA001008.

Luther, E.T., 1979. Geology of Hamilton County, Tennessee. Bulletin, 79. Tennessee Division of Geology, Nashville.

Meltzer, D.J., 1999. Human responses to Middle Holocene (Altithermal) climates on the North American Great Plains. Quaternary Research 52, 404–416.

Nordt, L.C., Boutton, T.W., Hallmark, C.T., Waters, M.R., 1994. Late Quaternary vegetation and climate change in Central Texas based on the isotopic composition of organic carbon. Quaternary Research 41, 109–120.

Nordt, L.C., Boutton, T.W., Jacob, J.S., Mandel, R.D., 2002. C_4 plant productivity and climate-CO_2 variations in south-central Texas during the Quaternary. Quaternary Research 58, 182–188.

Nordt, L., Wilding, L., Lynn, W.L., Crawford, C., 2004. Vertisol genesis in a humid climate in the coastal plain of Texas. Geoderma 122, 83–102.

PiPujol, M.O., Buurman, P., 1994. The distinction between ground-water gley and surface-water gley phenomena in tertiary paleosols of the Ebro basin, northeast Spain. Palaeogeography, Palaeoclimatology, Palaeoecology 110, 103–113.

Poore, R.Z., Dowsett, H.J., Verardo, S., Quinn, T.M., 2003. Millennial- to century-scale variability in Gulf of Mexico Holocene climate records. Paleoceanography 18 (2) 26–1:26–11.

Poore, R.Z., Quinn, T.M., Verardo, S., 2004. Century-scale movement of the Atlantic Intertropical Convergence Zone linked to solar variability. Geophysical Research Letters 31 (L12214). doi:10.1029/2004GL019940.

Richey, J.N., Poore, R.Z., Flower, B.P., Quinn, T.M., 2007. 1400 yr multiproxy record of climate variability from the northern Gulf of Mexico. Geology 35, 423–426.

Singer, M.J., Janitzky, P., 1986. Field and laboratory procedures used in a soil chronosequence study. US Geological Survey Bulletin 1648, 49 p.

Soil Survey Staff, 1996. Soil Survey Laboratory Information Manual: Soil Survey Investigations Report, 42. US Government Printing Office, Washington, D.C. Version 3.0.

Soil Survey Staff, 1998. Keys to Soil Taxonomy, 8th edition. US Government Printing Office, Washington, D.C.

Stichler, W., 1995. Interlaboratory Comparison of New Materials for Carbon and Oxygen Isotope Ratio Measurements. Reference and Intercomparison Materials for Stable Isotopes of Light Elements. International Atomic Agency, Vienna, Austria, pp. 67–74. IAEA TECDOC-825.

Stoops, G., 2003. Guidelines for Analysis and Description of Soil and Regolith Thin Sections. Madison, WI, Soil Science Society of America.

Vepraskas, M.J., Wilding, L.P., 1983a. Aquic moisture regimes in soils with and without low chroma colors. Soil Science Society of America Journal 47, 280–285.

Vepraskas, M.J., Wilding, L.P., 1983b. Albic neoskeletans in argillic horizons as indices of seasonal saturation and iron reduction. Soil Science Society of America Journal 47, 1202–1208.

Vepraskas, M.J., 1992. Redoximorphic Features for Identifying Aquic Conditions. Technical Bulletin, 301. North Carolina Agricultural Research Service, Raleigh, NC.

Vepraskas, M.J., 2001. Morphological features of seasonally reduced soils. In: Richardson, J.L., Vepraskas, M.J. (Eds.), Wetland Soils: Genesis, Hydrology, Landscapes, and Classification. Lewis Publishers, New York, pp. 163–182.

Vepraskas, M.J., Guertal, W.R., 1992. Morphological indicators of soil wetness. In: Kimble, J.M. (Ed.), Proceedings of the Eighth International Soil Correlation Meeting: Characterization, Classification, and Utilization of Wet Soils. USDA Soil Conservation Service, Lincoln, Nebraska, pp. 307–312.

Vepraskas, M.J., Wilding, L.P., Drees, L.R., 1994. Aquic conditions for soil taxonomy: concepts, soil morphology and micromorphology. In: Ringrose-Voase, A.J., Humphreys, G.S. (Eds.), Soil Micromorphology: Studies in

Management and Genesis. Developments in Soil Science 22. Elsevier Pub. Co., New York, pp. 117–131.
Wang, H., Follmer, L.R., Liu, J.C., 2000a. Isotope evidence of paleo-El Niño-Southern Oscillation cycles in loess–paleosol record in the central United States. Geology 28, 771–774.
Wang, Y., Amundson, R., Niu, X., 2000b. Seasonal and altitudinal variation in decomposition of soil organic matter inferred from radiocarbon measurements of soil CO_2 flux. Global Biogeochemical Cycles 14, 199–211.
Webb, R.S., Anderson, K.H., Webb, T., 1993. Pollen response-surface estimates of Late Quaternary changes in the moisture balance of the northeastern United States. Quaternary Research 40, 213–227.
Wilding, L.P., Tessier, D., 1988. Genesis of Vertisols: shrink–swell phenomena. In: Wilding, L.P., Puentes, R. (Eds.), Vertisols: Their Distribution, Properties, Classification and Management. Texas A & M University Printing Center, College Station, TX, pp. 55–81.
Yu, Z., Ito, E., 1999. Possible solar forcing of century-scale drought frequency in the northern Great Plains. Geology 27, 263–266.